Collodial Cluster Arrays by Electrohydrodynamic Printing

Sibel Korkut, Dudley A. Saville,[†] and Ilhan A. Aksay*

Department of Chemical Engineering, Princeton University, Princeton, New Jersey 08544-5263

Received July 22, 2008. Revised Manuscript Received September 1, 2008

A "stable" electrohydrodynamic jet is used to print arrays of colloidal suspensions on hydrophobic surfaces. Printed lines break up into sessile drops, and capillary forces guide the self-assembly of colloidal particles during the evaporation of the liquid, resulting in arrays of colloidal single particles or particle clusters depending on the concentration of the suspensions. The clusters differ from those formed in the absence of a substrate when the number of particles is larger than three. Multiple structures are found for the same number of particles.

I. Introduction

Organization of colloidal particles in well-defined arrangements is of interest for many applications including top-down production of new generation materials and photonic band gap crystals.[1,2] Patterning with colloidal particles typically involves multiple steps such as production of a suitable pattern on a mask or a substrate, introducing the colloidal particles or their precursors to the area to be patterned, and particle self-assembly under the influence of mechanical barriers, electrical and capillary forces, or chemical affinity.[3–7] In contrast, direct deposition of colloidal suspensions on a substrate through an orifice[8–16] (e.g., ink-jet printing) eliminates the need to use masks and hence sophisticated clean-room equipment. The conventional direct deposition techniques,[8,9] however, suffer in spatial resolution as a result of limitations on the orifice diameter of the nozzle, purposely kept large enough to prevent nozzle clogging. Here, we provide a method to produce self-assembled colloidal clusters in a single step using a recently developed electrohydrodynamic (EHD) printing technique.[10–16]

EHD printing (EHDP) utilizes "stable" electrified jets,[17,18] which are formed through cone–jet transition[19,20] to deploy liquids on moving surfaces in a well-controlled fashion. Cone–jet transition reduces the diameter of the jet by 2–3 orders of magnitude compared to the diameter at the exit of the nozzle and allows the production of patterns with less than 10 μm routinely and under appropriate conditions down to 100 nm.[10] Small feature sizes and accurate and fast printing make EHDP advantageous over current direct printing techniques in different aspects. Despite these advantages, there are two challenges that need to be addressed for successful EHDP: maintaining the stability of the EHD jet and controlling the stability of the liquid lines deployed on surfaces. The first challenge results from the amplification of axisymmetric and nonaxisymmetric (i.e., varicose and whipping) deformations of the jets due to their surface charge and small diameter.[21–23] To address this challenge, we have shown that stable EHD jets for printing can be obtained by various strategies involving either gas ionization, for example, by using small electrode separations or by changing the composition of the gas,[17] and/or adjustment of suspension properties, for example, by increasing its viscosity.[10]

The second challenge stems from the capillary break up of deployed lines of the liquid on surfaces. The extent of the capillary break up of these lines needs to be controlled in order to obtain arrays of intact lines or arrays of drops selectively. The capillary break up can be adjusted by controlling the evaporation time of the solvent and/or the break up time, which is a function of the wetting characteristics of the liquid on the substrate. Schiaffino et al.[24] have shown that as the contact angle of a fluid on a surface becomes smaller, the break up time becomes longer. When contact angles are acute and the contact lines are pinned, capillary break up can be completely eliminated. When the contact angles are obtuse, capillary instability develops regardless of the condition at the contact lines. Further, the pinning conditions of the contact line also affect the self-assembly of the particles. When pinning is negligible and lines break up to form sessile drops, evaporation-driven flow,[25] which is caused by contact line pinning, is not expected, and particles concentrate in smaller and smaller drops as the evaporation proceeds, whereas, in the case of pinning, evaporation-driven flow carries the particles to the contact lines and leads to a "coffee stain" behavior.[25]

* Corresponding author. E-mail: iaksay@princeton.edu.

† Deceased October 4, 2006.

(1) Lu, Y.; Yin, Y.; Xia, Y. *Adv. Mater.* **2001**, *13*, 415.

(2) Jiang, P.; Bertone, J. F.; Hwang, K. S.; Colvin, V. L. *Chem. Mater.* **1999**, *11*, 2132.

(3) Sun, Y.; Walker, G. C. *J. Phys. Chem. B* **2002**, *106*, 2217.

(4) Wang, D.; Mohwald, H. *J. Mater. Chem.* **2004**, *14*, 459.

(5) Aizenberg, J.; Braun, P. V.; Wiltzius, P. *Phys. Rev. Lett.* **2000**, *84*, 2997.

(6) Harris, D. J.; Hu, H.; Conrad, J. C.; Lewis, J. A. *Phys. Rev. Lett.* **2007**, *98*, 148301.

(7) Aizenberg, J.; Black, A. J.; Whitesides, G. M. *Nature* **1999**, *398*, 495.

(8) Morisette, S. L.; Cesarano, J., III; Lewis, J. A.; Dimos, D. B. U.S. Patent #6,454,972, 2002.

(9) Zhao, X.; Evans, J. R. G.; Edirisinghe, M. J.; Song, J-H. *J. Am. Ceram. Soc.* **2002**, *85*, 2113.

(10) Poon, H. F. Electrohydrodynamic printing. Ph.D. Thesis, Princeton University, 2002.

(11) Czaplewski, D. A.; Kameoka, J.; Mathers, R.; Coates, G. W.; Craighead, H. G. *Appl. Phys. Lett.* **2003**, *83*, 4836.

(12) Chen, C.-H.; Saville, D. A.; Aksay, I. A. *Appl. Phys. Lett.* **2006**, *88*, 154104.

(13) Chen, C.-H.; Saville, D. A.; Aksay, I. A. *Appl. Phys. Lett.* **2006**, *89*, 124103.

(14) Sun, D.; Chang, C.; Li, S.; Lin, L. *Nano Lett.* **2006**, *6*, 839.

(15) Lee, D.-Y.; Shin, Y.-S.; Park, S.-E.; Yu, T.-U.; Hwang, J. *Appl. Phys. Lett.* **2007**, *90*, 081905.

(16) Park, J.; Hardy, M.; Kang, S. J.; Barton, K.; Adair, K.; Mukhopadhyay, D. K.; Lee, C. Y.; Strano, M. S.; Alleyne, A. G.; Georgiadis, J. G.; Ferreira, P. M.; Rogers, J. A. *Nat. Mater.* **2007**, *6*, 782.

(17) Korkut, S.; Saville, D. A.; Aksay, I. A. *Phys. Rev. Lett.* **2008**, *100*, 034503.

(18) Korkut, S.; Aksay, I. A. *Phys. Rev. Lett.* **2008**, *101*, 059402.

(19) Cloupeau, M.; Prunet-Foch, B. *J. Aeros. Sci.* **1994**, *25*, 1021.

(20) de la Mora, J. F. *Annu. Rev. Fluid Mech.* **2007**, *39*, 217.

(21) Saville, D. A. *Phys. Fluids* **1971**, *14*, 1095.

(22) Hohman, M. M.; Shin, M.; Rutledge, G.; Brenner, M. P. *Phys. Fluids* **2001**, *13*, 2201.

(23) Reneker, D. H.; Yarin, A. L.; Fong, H.; Koombhongse, S. *J. Appl. Phys.* **2000**, *87*, 4531.

(24) Schiaffino, S.; Sonin, A. A. *J. Fluid Mech.* **1997**, *343*, 95.

(25) Deegan, R. D.; Bakajin, O.; Dupont, T. F.; Huber, G.; Nagel, S. R.; Witten, T. A. *Nature* **1997**, *389*, 827.
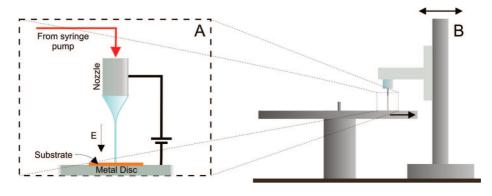
Figure 1. Schematic of the printing setup: (A) EHD jet formed between the dispenser nozzle and the substrate by continuously supplying the liquid through a syringe pump and applying an electric field between the nozzle and the metal disk. (B) Motion system composed of a rotary table and a linear motor that is located in the radial axis of the rotary table.

In this paper, we focus on EHDP of suspensions with polymeric solutions of polar fluids on a hydrophobic substrate. As a result of nonwetting conditions, the lines break up and yield arrays of colloidal clusters. Arrays of well-defined structures of colloidal clusters are not only of technological interest because of potential applications such as superhydrophobic surfaces,[26] optoelectronic devices,[27,28] seeds for building larger three-dimensional (3D) structures, and lithographical masks,[29] but also of scientific interest as analogues of atomic clusters.[30−32] Manoharan et al.[33] demonstrated the production of novel colloidal clusters by evaporating the solvent of a suspension emulsified in another liquid. The resulting clusters were unique in the sense that the packings depended on the number of particles within the cluster. Lauga et al.[34] modeled the clustering described by Manoharan et al. as a surface energy minimization process during the evaporation of the liquid as the liquid−vapor interface deforms around the protruding colloidal particles. For a small number of particles, the configuration of the particle clusters was shown to always be the same, independent of the size of the particles. In the presence of a substrate, however, the numerical simulations[35] predict that more than one packing arrangement is possible for a given number of particles.

Contrary to the case of packings in emulsions, experimental data on the packing of a small number of particles on a substrate are scarce, possibly due to the need to deploy minute volumes of suspensions. Efforts with inkjet printing of very dilute colloidal suspensions on hydrophobic surfaces have been limited to large clusters,[36−38] with face-centered cubic crystals, which are characteristic structures of the bulk systems.[39,40] The only experimental work on the packing of a small number of particles on a substrate to produce "colloidal molecules"[41] was reported

by Masuda et al.,[42] which involved a two-step process for the production of regular arrays of particle clusters by first prepatterning the substrate with circular hydrophilic regions. The clusters produced on these surfaces indeed differed from the ones produced without a substrate.

In the following sections, we first demonstrate the utility of EHDP for producing regular arrays of microdrops, then we use this technique for the production of colloidal clusters on surfaces as a rapid and single step process; finally, we compare our experimental results with the simulations of Schnall-Levin et al.[35] and discuss the mechanism of self-assembly for the clusters formed.

II. Experimental Section

Suspensions of polystyrene microspheres (5.7 μm carboxylate-modified latex particles from Interfacial Dynamics Corp. or 3.1 μm amino-modified microspheres from Bangs Laboratories, Inc.) in solutions of polyethylene oxide (PEO, MW: 300 000) were used in printing. The concentration of PEO was adjusted to be between 0.015 and 0.023 g/mL for 6−15% particles in the suspension by volume. The lower limit of the polymer concentration is determined by the stability of cone and jet. A steady cone and a stable jet could not be sustained at low PEO concentrations ($\leq$0.010 g/mL) for volumetric flow rates <2.5 mL/h, which results in hundreds of particles per drop. On the other hand, when the PEO concentration was high ($\geq$0.022 g/mL) and the colloid concentration was low (<2% by volume), the particles were immobilized by the PEO before the capillary forces required for their self-assembly became effective.

In the experimental work, we first prepared a concentrated solution of PEO (8.86 g of PEO in 100 mL of solvent) in ethanol and deionized water at a 1:1 volume fraction. Then, the as-received particle suspensions were centrifuged, and, depending on the desired final concentration, the supernatant was replaced by an appropriate amount of deionized water, ethanol, and concentrated PEO solution. The substrates were prepared from gold-coated silicon wafers. After being cut to approximately 1 $\times$ 1 cm² size squares, their surfaces were wet with a 2 mM 1-hexadecanethiol solution in ethanol with the help of a cotton swab. This was followed by drying the surface under a flow of nitrogen, rinsing the substrate with ethanol, and drying it under a flow of nitrogen.

EHDP was done using a needle-plate electrode system (Figure 1). The upper electrode was a stainless steel Hamilton needle (gauge 21−26, i.e., inner diameter/outer diameter: 0.51/0.82 to 0.34/0.64 mm). The lower electrode was a brass disk attached to a rotary motor (M 3353 motor, Baldor Electric Co., Fort Smith, AR) with a frequency controller (model FR-U11OW-0.1K-UL, Mitsubishi Electric Corp., Japan). The nozzle was fixed on a Plexiglas part, attached to a custom-built linear motor (M-1715-1.5 S linear stage with IP404C and an MX-CC200-01 human−machine interface unit, Intelligent Motion Systems, Inc., Rocky Hill, CT). Before starting
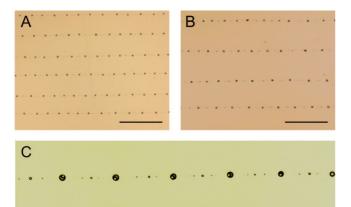
(26) Li, Y.; Huang, X. J.; Heo, S. H.; Li, C. C.; Choi, Y. K.; Cai, W. P.; Cho, S. O. *Langmuir* **2007**, *23*, 2169.

(27) Nam, H. J.; Jung, D.-Y.; Yi, G.-R.; Choi, H. *Langmuir* **2006**, *22*, 7358.

(28) Veinot, J. G. C.; Yan, H.; Smith, S. M.; Cui, J.; Huang, Q.; Marks, T. J. *Nano Lett.* **2002**, *2*, 333.

(29) Burmeister, F.; Schafle, C.; Mathes, T.; Bohmisch, M.; Boneberg, J.; Leiderer, P. *Langmuir* **1997**, *13*, 2983.

(30) Frank, F. C. *Proc. R. Soc. London A* **1952**, *215*, 43.

(31) Nelson, D. R.; Spaepen, F. *Solid State Phys.* **1989**, *42*, 1.

(32) Schenk, T.; Holland-Moritz, D.; Simonet, V.; Bellissent, R.; Herlach, D. M. *Phys. Rev. Lett.* **2002**, *89*, 075507.

(33) Manoharan, V. N.; Pine, D. J.; Elsesser, M. T. *Science* **2003**, *301*, 483.

(34) Lauga, E.; Brenner, M. P. *Phys. Rev. Lett.* **2004**, *93*, 238301.

(35) Schnall-Levin, M.; Lauga, E.; Brenner, M. P. *Langmuir* **2006**, *22*, 4547.

(36) Ko, H.-Y.; Park, J.; Shin, H.; Moon, J. *Chem. Mater.* **2004**, *16*, 4212.

(37) Kim, S.-H.; Lim, J.-M.; Jeong, W. C.; Choi, D.-G.; Yang, S.-M. *Adv. Mater.* **2008**, *20*, 3211.

(38) Wang, D.; Park, M.; Park, J.; Moon, J. *Mater. Res. Soc. Symp. Proc.* **2006**, *901E*, 0901-Ra16-10-Rb16-10.

(39) Shih, W. Y.; Aksay, I. A.; Kikuchi, R. *J. Chem. Phys.* **1987**, *86*, 5127.

(40) Shih, W. Y.; Shih, W.-H.; Aksay, I. A. *J. Chem. Phys.* **1989**, *90*, 4506.

(41) Blaaderen, A. *Science* **2003**, *301*, 470.

(42) Masuda, Y.; Itoh, T.; Koumoto, K. *Adv. Mater.* **2005**, *17*, 841.

Figure 2. Optical microscope images of patterns on a hexadecanethiol-coated surface produced by EHDP of (A) a PEO solution in ethanol and water at a 0.15 mL/h flow rate, 3 mm electrode separation, and 0.57 kV/mm nominal electric field, and (B) a suspension of 3.1 μm polystyrene particles in the PEO solution at a 0.15 mL/h flow rate, 2 mm electrode separation, and 0.57 kV/mm nominal electric field. (C) A higher magnification image of the pattern shown in B demonstrating single particle array of 3.1 μm particles. The scale bars designate 200 μm in both A and B.

the printing experiments, one of the substrates was placed on the rotary table and fixed using an electrically conducting (typically copper) tape. Experiments involved feeding the suspension to the nozzle through a Teflon tube using a syringe pump (model Harvard 33 Twin Syringe Pump, Harvard Apparatus, Holliston, MA). Upon application of sufficiently high potential differences (model 620A, Trek, Inc., Beaverton, OR) between the electrodes, typically on the order of 1−5 kV, a thin jet was formed. Electrode separation was kept between 2 and 5 mm, while the volumetric flow was between 0.1 and 0.6 mL/h. As the nozzle moved in the radial direction of the rotating table, spiral-shaped patterns were formed on the table. The patterns appeared linear on the substrate in optical or electron microscopic studies because of the small size of the substrate compared to the radius of the rotary table. The velocities of the tables were chosen depending on the desired distance between each pattern, as well as the need for stretching of the polymeric jet (in this work, 1−2 rps and 250−300 μm/s).

III. Results and Discussion

We first focus on the properties of the islands formed by EHDP on hydrophobic surfaces. In the second part, we discuss the self-assembly and the structure of particle clusters produced from suspensions deployed on these surfaces.

Break Up of Printed Lines. EHDP on hexadecanethiol-coated surfaces with (i) a PEO solution and (ii) a suspension of polystyrene particles (3.1 μm in diameter at 0.77% by volume) in a PEO solution yielded the patterns shown in Figure 2A,B, respectively. (Solution used for Figure 2A had 0.026 g/mL PEO, 85% by volume water and 15% by volume ethanol. Solution used for Figure 2B and C had 0.024 g/mL PEO, 85.4% by volume water, 13.8% by volume ethanol, and 0.8% by volume polystyrene particles.) Both patterns were produced under the same printing conditions except for the velocity of the linear motor. Although the jet was deployed on the surface as a continuous "line", the deployed liquid filament was unstable and broke up into drops since the contact angle[43] was greater than 90° and the contact lines were not pinned.[44,45] This break up is due to a two-dimensional (2D)

version of Rayleigh instability caused by capillarity.[24,46] When the instability sets in, the lines bulge in some parts and thin down in between the bulges. Main drops form from the bulges, whereas the satellite drops form as a result of detachment of the thin section of the liquid from the bulges. The diameters of the main islands shown in Figure 2A,B are 7.5 ± 0.6 μm and 7.9 ± 0.7 μm, respectively. The islands align in rows that make less than a 1° angle with each other, whereas particles deviate ± 3.5 μm from a straight line since colloidal particles are located randomly within the polymer residues (Figure 2C). The average separations between the main islands in each row in Figure 2A,B are 56.8 ± 7.5 and 76.2 ± 16.4 μm, and the distances between the rows are 95.2 ± 6.6 and 141 ± 7.0 μm, respectively.

In Figure 2C, two generations of satellite islands between the main islands are visible. The presence of these satellite islands indicates a secondary break up of the long bridges between the main drops, which form possibly because the wavelength of the disturbances is long.[47] Both centered and off-centered satellite drops exist between the main drops either as a result of the differences in the initial pinch off location of the satellite drops from the main drops or as a result of the pinning of the satellite drops on the heterogeneities of the substrate. The size of the main drops and the distribution of colloidal particles are affected by the satellite drops, and thus their occurrence introduces undesirable effects. An effort to eliminate the satellites was not made in this study.

There are three main geometrical features that define the arrays: (i) the size of individual islands produced by the drops, (ii) the separation between the islands within a row, and (iii) the distance between the rows of the islands. The wavelength of the fastest growing disturbance defines the center-to-center separation between the main drops. We use the linear axisymmetric stability theory for a viscous jet[48] to estimate the expected dominant wavelength because of the lack of a theory for capillary instability of viscous liquid filaments on substrates. The initial half-width of the liquid on the substrate (assuming that the contact angle is 90°) is found by using the mass conservation[49] as $r \sim (2Q/\pi v)^{1/2}$. In this expression, Q is the volumetric flow rate, and v is the linear velocity of the table. Under the experimental conditions leading to the patterns shown in Figure 2, the lines are expected to be ∼9.7 μm wide. Thus, the fastest growing wave for a jet[48] of 9.7 μm diameter is ∼60.7 μm long.[50] This value is fairly close to the experimentally observed island-to-island separation of 56.8 ± 7.5 μm (Figure 2A) for the PEO solution without the particles. Hence, despite the existence of the substrate, the theory for a jet break up provides a good guideline for controlling the center-to-center separation between the individual islands. The fact that the theory for a free-standing viscous jet works well points to the weak influence of the substrate due to a high contact angle (∼90°) and no significant pinning.

(43) The receding contact angle of water on this substrate is between 96° and 99°. Drelich, J.; Wilbur, J. L.; Miller, J. D.; Whitesides, G. M. *Langmuir* **1992**, *12*, 1913.

(44) Dettre, R.; Johnson, R. In *Contact Angle, Wettability and Adhesion*; Fowkes, F. M., Ed.; Advances in Chemistry Series, No. 43; American Chemical Society: Washington, DC, 1964.

(45) Yu, H.; Soolaman, D. M.; Rowe, A. W.; Banks, J. T. *Chem. Phys. Chem.* **2004**, *5*, 1035.

(46) McCallum, M. S.; Voorhees, P. W.; Miksis, M. J.; Davis, H. S.; Wong, H. *J. Appl. Phys.* **1996**, *79*, 7604.

(47) Eggers, J. *Rev. Mod. Phys.* **1997**, *69*, 865.

(48) Chandrasekhar, S. *Hydrodynamic and Hydromagnetic Stability*; Clarendon Press: Oxford, 1961; Chapter 12, pp 540−543.

(49) Time to deploy one wavelength long liquid line is λ/v. The total volume of the liquid deployed during this time is $Q(\lambda/v)$. Initial half width of the liquid on the substrate is obtained by equating the volume of a half cylinder with length λ and radius r, $1/2\pi r^2 \lambda$, to the deployed volume during this time. Similarly, the radius of the spherical cap is found by equating the deployed volume to the volume of a spherical cap: $4/6\pi R^3$.

(50) The dimensionless number, $\gamma r g/\mu^2$, where γ, r, g, and μ are the surface tension, radius, gravitational acceleration, and viscosity of the solution (for our polymeric solution, ∼8 cP, based on its PEO concentration), respectively, is found as 5.5. Using this value, the dimensionless wavenumber, corresponding to the fastest disturbance growth rate, is read from Figure 129 of ref 48 by Chandrasekhar as ∼0.5. Wavelength is calculated from $2\pi r/0.5$ as 60.7 μm.

However, the experimental results deviate more from the prediction in the case of suspensions. Further, the standard deviation of the center-to-center distance from the average also increases in the case of suspensions. We attribute these deviations to the effect of the particles on the break up by modifying the fluid flow during the break up process.

Because the solvent evaporates from the deployed lines, break up of the printed lines also requires that the time scale for the instability must be shorter than the time scale for evaporation. When the evaporation rate is higher than a critical value, it is possible to prevent the break up and keep the printed lines intact.[10] Using the theory for the stability of a continuous jet, the time scale for the instability[48] can be found by using the scaling for the inverse of the instability growth rate as $t_c \sim r^2\rho/\mu$, where r is the radius, ρ is the density, and μ is the viscosity of the liquid. The evaporation time scales[51] as $t_e \sim r^2\rho/DC$, where D and C are the diffusivity of the solvent molecules and the saturation concentration of the solvent in air, respectively. Assuming that the break up time will scale the same as a jet of the same diameter, the time for break up is $\sim 15\ \mu s$, and the time for evaporation is $\sim 20\ ms$. Because $t_c \ll t_e$, it is safe to conclude that the deployed lines break up "instantaneously", and the effect of changes in the dimensions and the physical properties, such as viscosity due to evaporation on the break up dynamics, is negligible. Essentially, the process can be thought of as capillary break up of a nonvolatile liquid and evaporation from the sessile drops.

The length of the fastest growing wave, λ, and the cross-sectional area of the liquid at the time of the break up defines the initial volume of an island as $Q\lambda/v$. The ratio of gravitational forces to surface tension forces, i.e., Bond number,[52] for the sessile drops produced as a result of capillary break up is $\sim 10^{-5}$. Hence, the maximum size of the islands prior to the evaporation of the solvent can be found by assuming that the shape of the drops is not influenced by the gravity and they take the shape of a spherical cap:[49] $R \sim (3Q\lambda/2v\pi)^{1/3}$. The final size of the islands is determined depending on at what stage of the evaporation the contact line gets pinned, how much of the liquid gets consumed by the satellite drops, and how many particles are in an island. For example, in the patterns shown in Figure 2A, the initial diameter of the drops after break up is $20.4\ \mu m$, whereas their final diameter is $7.5\ \mu m$. Not surprisingly, the inclusion of particles in the printing solution increases the size of the islands both by the existence of particles as well as the increase in the island-to-island separation (Figure 2B).

A straight EHD jet with negligible bending enables the printing of parallel rows. Separation between the rows, d, is controlled by the angular velocity of the rotary table and the radial velocity of the linear motion. It is given by $d = V_r/V_\theta$, where V_r and V_θ are the radial and angular velocities, respectively. Given this relationship, the expected values of d for the patterns shown in Figures 2A and B are 100 and 150 μm. Experimental measurements agree well with the expectations, and the difference is possibly due to the limited accuracy of the equipment and slight bending of the jet. There is a statistical variation of the number of particles per island, similar to the drop and place technique.[12,13] Despite that, the concentration of colloids was adjusted to have one particle per island, and Figure 2C shows that only five islands (on the left) out of six contain a particle. Figure 3 gives the distribution of the number of particles per island for an array that is expected to have 3.8 particles per island based on the concentration of the suspension. The shape of the distribution
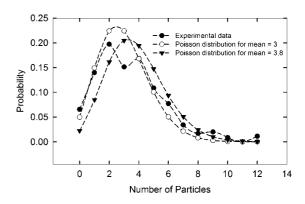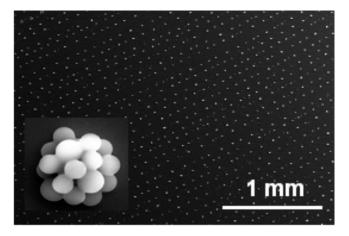
(51) Birdi, K. S.; Vu, D. T.; Winter, A. *J. Am. Chem. Soc.* **1989**, *93*, 3702.
(52) Probstein, R. F. *Physicochemical Hydrodynamics, An Introduction*; Butterworth Publishers: Stoneham, MA, 1989; Chapter 9, p 278.
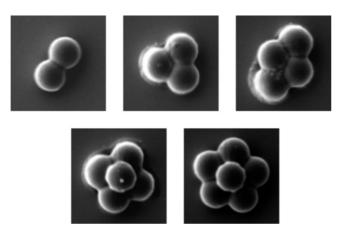

Figure 3. Statistical distribution of number of particles within each cluster found using a total of 350 islands.

Figure 4. A scanning electron microscope image of arrays of self-assembled 5.7 μm polystyrene particles after EHDP of a suspension at a 0.55 mL/h flow rate, 2.8 mm electrode separation, and 0.56 kV/mm nominal electric field on a hydrophobic substrate. The inset shows a higher magnification of one of the clusters, which appears as white points in the lower magnification image.

agrees with a Poisson distribution except for the probability of finding three particles. The probabilities for smaller number of particles are higher than what is predicted by the Poisson distribution with an average of 3.8, and it is closer to the distribution for which the average is 3. This is due to the reduction in the average number of particles per island since some of the particles are consumed by the satellite islands. The reason for the disagreement in the probability of finding three particles is unclear. One possible explanation for this is the existence of doublets in the suspension, which decrease the probability of finding an odd number of particles per cluster, an effect that is expected to be more pronounced for a small number of particles per cluster.

Clusters of a Small Number of Particles. Figure 4 demonstrates arrays produced with a concentrated (15% of 5.7 μm polystyrene) suspension. After the capillary break up, particles self-assemble[53] in a "berry-like" 3D structure (inset of Figure 4). The self-assembly is controlled by the capillary forces on the particles. Other effects such as gravitational force and the evaporation-driven flow[25] are negligible: during the time of evaporation, particles are expected to move less than a micrometer as a result of gravity,[54] and the observation of tracer particles in an evaporating sessile drop on a substrate prepared the same way revealed no preferential motion of particles toward contact lines.

(53) Whitesides, G. M.; Grzybowski, B. *Science* **2002**, *295*, 2418.

Figure 5. The most common structures of colloidal clusters, composed of different numbers of 5.7 μm diameter polystyrene particles, produced on a 1-hexadecanethiol-coated gold surface from EHDP of the colloidal suspension.

The root-mean-square distance traveled by the particles during the time of the evaporation is on the order of tens of nanometers.[55] Therefore, unless they are already very close, particles are not expected to reach the air−liquid interface until the volume of the liquid is less than the amount required to completely enclose the particles. From this point on, the interface deforms to satisfy the wetting conditions at the particle surface, and immersion-type capillary forces[56] become active. As the capillary energy exceeds the trapping energy at the interface, particles configure themselves on the basis of the net force they are under.

One of the requirements for the formation of clusters shown in Figure 4 is the absence of bond formation between the particles at the onset of contact. When particles are bonded, hollow colloidosomes[57] are formed rather than packed clusters. Particles used for concentrated suspensions in this work had a 1.6 C/m^2 surface charge density due to the carboxylate groups on their surface. Calculations[58] show that our particles are electrostatically stabilized, hence the particle−particle interactions are expected to be reversible unless the polymer residue acts as a glue at the final stages of solvent evaporation.

Figure 5 shows the most frequently observed structures from EHDP of a suspension containing 6% particles (5.7 μm) by volume on a hexadecanethiol-coated gold surface. A minimum of 150

clusters was investigated for each number of particles per cluster. The clusters shown in Figure 5 for 2, 3, 4, 5, and 6 particles occurred 100, 86, 48, 40, and 35% of the time, respectively. Some of the clusters included in these percentages had imperfections such as asymmetrical spacing for the lower group of particles for the case of 5 and 6 particles per cluster. Particles in each cluster appear permanently deformed, filling all the interstitial regions. We attribute this deformation to capillary forces. The structure of the clusters formed on the substrate is different than what has been reported[33] previously as a result of evaporation from a fully spherical drop in the absence of a substrate (Figure 5) with the exception of the two and three particle cases. The existence of the substrate affects the packing of the particles in two ways: (i) by introducing capillary interactions between particles and the substrate, and (ii) by limiting the height of the drop and the available area for packing of particles at the interface. Capillary interactions between particles and the substrate differ from capillary interactions between two particles, not only in magnitude but also in direction. Capillary interactions between the particles and the substrate can be either attractive or repulsive[56] depending on the contact angle of the particle and the substrate with the liquid, whereas the capillary interactions between chemically identical particles are always the attractive type. Therefore, in the presence of a substrate, forces experienced by the particles vary depending on their location on the drop, which breaks the spherical symmetry. Height limitations of the drop may cause a region around the liquid−substrate contact line to be inaccessible to the particles. For this reason, even if the liquid−substrate contact angle is 180°, the particle packings are not necessarily going to be identical to those formed from a substrate-free drop.

Our experiments show that, unlike the clusters that form as a result of evaporation from a fully spherical drop,[33] there is more than one possible structure for the same number of particles per cluster in the presence of a substrate. There are two possible reasons for the observed degeneracy on the substrate. Either the existence of the substrate increases the number of possible configurations as predicted by Schnall-Levin et al.,[35] or some of the particles get kinetically trapped in nonequilibrium positions during evaporation of the solvent. The agreement of the structure of our five-particle cluster (Figure 5) with the one demonstrated by Masuda et al.[42] supports the former, at least for the five-particle cluster.

The most common structures for five- and six-particle clusters shown in Figure 5 are also identical to the pyramid structures found from simulations[35] based on surface energy minimization, despite the fact that the calculations[35] were done for particles that had a 90° contact angle with the liquid, whereas, in our case, particles are hydrophilic because of the presence of carboxylate groups on their surfaces.[59] The ring structures, for which all the particles make a ring on the same plane, are not observed. Instead, there are clusters with a single layer, which possibly formed as a result of collapse of ring structures, in agreement with the predictions.[35]

IV. Summary and Conclusions

EHDP of colloidal particle arrays in a single step is demonstrated by utilizing capillary break up followed by self-assembly. A range of arrays, from single particles to 3D colloidal clusters, is produced by varying the concentration of the suspension used in printing. The number of particles per cluster

(54) Time for evaporation of a sessile drop scales as $t_e \sim \rho R^2/4CD$ (ref 48), and the settling velocity of the particles scales as $U_s \sim 2(\rho_p - \rho)gR_p/9\mu$. Here, $\rho, \rho_p, g, R, R_p, \mu \; C$, and D are the density of the liquid and the particle, gravitational acceleration, radii of the drop and the particle, viscosity of the liquid, saturation concentration of the liquid, and the diffusivity of its vapor in air, respectively. Substituting the values representing experimental conditions, the settling velocity for 5.7 μm polystyrene particles is found to be ∼0.16 μm/s. The time of evaporation for a drop with a 30 μm diameter is ∼0.1 s. Hence, during the time of evaporation, particles are expected to settle at a ∼16 nm distance due to gravity.
(55) The root mean displacement of the particles is given as $(x^2)^{1/2} = (2D_p t)^{1/2}$, where D_p is the diffusivity of the particle in the liquid defined as $D_p = (kT/6\pi\mu R_p)$. In these expressions, t is time, k is the Boltzmann constant, and T is the temperature. Using the time as the evaporation time defined above, the root mean square distance at room temperature is calculated as ∼51 nm for 5.7 μm particles.
(56) Kralchevsky, P. A.; Nagayama, K. *Adv. Colloid Interface Sci.* **2000**, *85*, 145.
(57) Dinsmore, A. D.; Hsu, M. F.; Nikolaides, M. G.; Marquez, M.; Bausch, A. R.; Weitz, D. A. *Science* **2002**, *298*, 1006.
(58) We calculated the sum of the electrostatic and the van der Waals energies for spheres with a constant surface charge density (for the calculations, see eq 4.10.11 in Russel, W. B.; Saville, D. A.; Schowalter, W. R. *Colloidal Dispersions*; Cambridge University Press: Cambridge, 1989, and eq 11.3.12 in Hunter, R. J. *Foundations of Colloidal Science*, 2nd ed.; Oxford University Press; New York, 2002). By taking the carbonic acid dissociation in water into account, the Debye length is found as 173 nm for 5.7 μm diameter polystyrene particles with a surface charge density of 1.6 C/m^2. The total potential of the particles has a shallow secondary minimum of ∼0.029 kT, which can be easily overcome by the thermal energy. This is followed by a steep repulsive energy barrier of thousands of kT, which prevents the particles from reaching the primary minimum.

(59) Holmes-Farley, S. R.; Bain, C. D.; Whitesides, G. M. *Langmuir* **1998**, *4*, 921.

in an array shows a statistical distribution, and there are satellite drops between the main clusters. These issues can be resolved by deploying suspensions by a pulsed EHDP technique[13] with a gating system. The existence of the substrate influences the structure of the colloidal clusters as a result of additional geometrical requirements and different capillary interactions between the particle and the substrate. Multiple configurations are observed for the same number of particles. Although the experimental conditions differ, some of the structures observed here agree with the ones found theoretically by Schnall-Levin et al.[35] and experimentally by Masuda et al.[42] Further experiments are needed to understand the influence of particle and substrate contact angles on the structure of the colloidal clusters.